Received: *June 13, 2000*, Accepted: *September 13, 2000*
Revised: *August 17 , 2000*

Searching for narrow graviton resonances with the ATLAS detector at the Large Hadron Collider

Ben C. Allanach
DAMTP, University of Cambridge
Wilberforce Road, Cambridge CB3 0WA, UK
E-mail: b.c.allanach@damtp.cam.ac.uk

Kosuke Odagiri
Rutherford Appleton Laboratory, Chilton
Didcot OX11 0QX, UK
E-mail: odagiri@hep.phy.cam.ac.uk

M. Andy Parker and Bryan R. Webber*
Cavendish Laboratory, University of Cambridge
Madingley Road, Cambridge, CB3 0HE, UK
E-mail: parker@hep.phy.cam.ac.uk, webber@hep.phy.cam.ac.uk

Abstract: A spectrum of massive graviton states is present in several recent theoretical models that include extra space dimensions. In some such models the graviton states are well separated in mass, and can be detected as resonances in collider experiments. The ability of the ATLAS detector at the Large Hadron Collider to identify such states and measure their properties is considered, in the case that the resonances are narrow compared to the experimental resolution. The discovery limits for the detection of the decay mode $G \to e^+e^-$ are derived. The angular distribution of the lepton pair is used to determine the spin of the intermediate state. In one specific model, the resonance can be detected up to a graviton resonance mass of 2080 GeV, while the angular distribution favours a spin-2 hypothesis over a spin-1 hypothesis at 90% confidence for resonance masses up to 1720 GeV.

Keywords: Extra Large Dimensions, Beyond Standard Model, Hadronic Colliders.

*Theory Division, CERN, 1211 Geneva 23, Switzerland.

JHEP09(2000)019

Contents

JHEP09(2000)019

1. Introduction

The recently proposed localized gravity model of Randall and Sundrum [1] has aroused great theoretical interest, and many possible extensions and elaborations of this type of theory are being discussed in the literature [2]. The model was initially motivated because it solved the weak-Planck scale hierarchy via an exponentially suppressed warp factor in a non-factorisable geometry. Despite possible problems with negative tension branes and stability in some of the frameworks, these problems are solved in other models. For now, we ignore the details of particular models and concentrate on a measurement that should apply to a broad class of the models. Such scenarios are characterised by the existence of a series of graviton excitations, which may be detectable at present and future colliders. In some cases these excitations may be sufficiently well spaced to be detected as individual resonances.

This work will discuss the possibility of detecting such graviton resonances in as model independent a way as possible, using the scenario of [1] as a guide. However, the results derived do not depend on the validity of this particular scenario, but can be applied to any model giving rise to narrow graviton resonances.

In the scenario of [1] the massive graviton excitations couple with equal strength to the visible sector [3]. However, the higher modes being suppressed by the falling parton distribution functions, we consider only the lightest mode. This does not in any way affect the generality of our approach, as our analysis can be applied to any such resonances, including the higher modes, so long as the resonances are narrow and sufficiently separated from the other modes. This is in contrast to studies in which many excitations, each with small coupling, contribute to some scattering process [4].

An event generator capable of simulating the production and decay of spin-2 resonances has been developed. This generator is an extension of the HERWIG 6.1 [5] simulation package. The generated events are passed through the ATLAS fast simulation (ATLFAST [6]), in order to give a realistic description of detector resolution and efficiency. The decay channel $G \to e^+e^-$ is chosen for study, since the ATLAS detector has excellent energy and angular resolution for high energy electrons, and the Standard Model background comes dominantly from the well-understood Drell-Yan process. The observable cross section for this process is considered first, and limits on the discovery reach of ATLAS, based simply on the ability to detect the resonance above the Standard Model background, are derived. The angular distribution of the decay products is then considered, in order to study the ability of the detector to determine the spin of the resonance.

2. The event generator

In the model of [1], a 5-dimensional non-factorizable geometry is used, with two 3-branes of opposite tension. A graviton Kaluza-Klein spectrum is created, with a scale $\Lambda_\pi = \bar{M}_{\rm Pl} e^{-kr_c\pi}$, where $\bar{M}_{\rm Pl}$ is the reduced effective 4-D Planck scale, r_c is the compactification radius of the extra dimension, and k is a scale of the order of the Planck scale. The geometrical exponential factor (dubbed the "warp factor") generates TeV scales from fundamental Planck scales and hence offers a solution to the hierarchy problem, if $kr_c \approx 12$. The masses of the graviton resonances are given by $m_n = kx_n e^{-kr_c\pi} = x_n(k/\bar{M}_{\rm Pl})\Lambda_\pi$ where x_n are the roots of the Bessel function of order 1. The couplings of the massive resonances are given by $1/\Lambda_\pi$. The properties of the model are determined by the ratio $k/\bar{M}_{\rm Pl}$. We have chosen a value of 0.01 (at the bottom of the range suggested in [3]) for this ratio, which according to [7], is on the edge of 95% exclusion for a first graviton excitation mass of less than 2000 GeV. Thus, we assign a low coupling constant to the gravitons, and hence obtain a conservative estimate of the production cross section. This choice leads naturally to narrow resonances. This test scenario is used to illustrate the potential physics reach.

The implementation of the resonance is largely model independent, depending only on a universal coupling to the Standard Model fields. This is generally the case for models deriving from extra dimensions, and the effective lagrangian is given at first non-trivial order in $1/\Lambda_\pi$ as:

$$\mathcal{L}_I = -\frac{1}{\Lambda_\pi} h^{\mu\nu} T_{\mu\nu} \,, \tag{2.1}$$

where $h^{\mu\nu}$ is the spin-2 field and $T_{\mu\nu}$ is the energy-momentum tensor of the Standard Model fields. Here, we consider only the production and measurement of the lightest

JHEP09(2000)019

Process	Distribution
$gg \to G \to e^+e^-$	$1 - \cos^4\theta^*$
$q\bar{q} \to G \to e^+e^-$	$1 - 3\cos^2\theta^* + 4\cos^4\theta^*$
$q\bar{q},\, gg \to V \to e^+e^-$	$1 + \alpha\cos^2\theta^*$
$q\bar{q},\, gg \to S \to e^+e^-$	1

Table 1: Angular distributions in graviton (G), vector (V) and scalar (S) boson production and decay. $\alpha = 1$ in Standard Model processes.

massive graviton excitation. We note however [1], that other heavier resonances are expected. In the case we consider here, they are well split in mass and hence the lightest resonance will be produced dominantly.

The decay $G \to e^+e^-$ is treated in the HERWIG implementation as a $2 \to 2$ process, consisting of the two hard production subprocesses $q\bar{q} \to e^+e^-$ and $gg \to e^+e^-$. For the $q\bar{q} \to e^+e^-$ channel we do not consider interference with the Standard Model Drell-Yan subprocesses as the interference is negligible for our purposes. The code is available from the authors on request.

For calculating the matrix elements and the total decay width of the graviton resonance, we made use of the results in [8, 9, 10]. We carried out our calculations both by hand and by using HELAS [11] incorporating subprograms with spin-2 particles [12]. Our implementation of the decay widths corrects a typographical error in [8] for the decay into heavy vector bosons but this has only a small effect on the total decay width.

$$\Gamma(G \to VV) = \delta \frac{m_G^3}{40\pi\Lambda_\pi^2}(1 - 4r_V)^{1/2}\left(\frac{13}{12} + \frac{14}{3}r_V + 4r_V^2\right), \tag{2.2}$$

where, as in [6], $\delta = 1/2$ for identical particles and $r_V = m_V^2/m_G^2$.

The angular distributions of the possible subprocesses, in the centre-of-mass frame of the resonance, are shown in table 1. Here θ^* is the angle between the decay electron and the beam direction in the dilepton centre-of-mass frame. The spin-2 distributions contrast strongly with the angular distributions resulting from spin-1 or scalar resonances. These distributions are shown in figure 1.

3. Detection of the graviton resonance

The process $pp \to G \to e^+e^-$ must be detected above the background from the Standard Model processes $pp \to \mathrm{Z}/\gamma^* \to e^+e^-$. Samples of events were generated for a single graviton excitation with a mass ranging from 500 GeV to 2.2 TeV. The masses and widths of the graviton resonances are given in table 2, as they are computed with the model parameters given above. The table also shows the cross-section times branching ratio $\sigma \cdot B$ in the test model and the width of the resonance reconstructed

JHEP09(2000)019

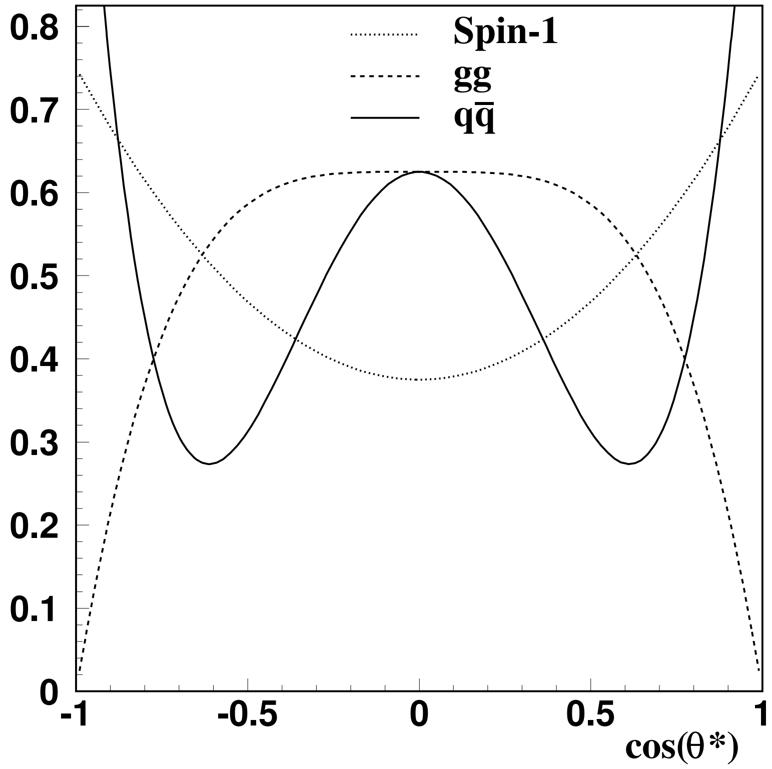

Figure 1: The normalised theoretical angular distributions for $gg \to G \to e^+e^-$ (dashed curve), $q\bar{q} \to G \to e^+e^-$ (solid curve) and $q\bar{q} \to Z/\gamma^* \to e^+e^-$ (dotted curve).

after the ATLAS detector simulation. In all the cases studied, the true width of the resonance is much smaller than the gaussian experimental resolution Γ_m and can be neglected. Hence the results are valid for any model in which this condition is met. In our test model, this is the case for $k/\bar{M}_{\rm Pl} < 0.06$, at which point the width is approximately equal to the experimental resolution, and the cross section is 36 times larger than we have assumed. For larger values of $k/\bar{M}_{\rm Pl}$, the very high signal cross sections would overwhelm the Standard Model background, making the resonance very easy to detect, and the spin simple to determine, even with a large width.

For each mass point, having determined the observed resonance width Γ_m, a mass window is defined as $\pm 3\Gamma_m$ around the graviton mass. The Drell-Yan cross-section inside this mass window is then calculated using the HERWIG 6.1 event generator [5]. The number of background events expected in the mass window is then computed, for an integrated luminosity of $100\,\text{fb}^{-1}$, corresponding to one year of LHC running at design luminosity. The ATLFAST simulation of the ATLAS detector is used to compute the acceptance for the process, which is dominated by the pseudorapidity (η) coverage of the tracker, $|\eta| < 2.5$. Cuts are also made on the isolation of the electrons to account for the effect of nearby hadrons on the detection efficiency. In addition to the cuts imposed by ATLFAST, a tracking efficiency of 90% was applied to each electron, to allow for track reconstruction losses which are

JHEP09(2000)019

m_G (GeV)	Γ_G (GeV)	Γ_m (GeV)	$\sigma \cdot B$ (fb)
500	0.068	3.53	281.9
1000	0.141	6.02	11.0
1500	0.213	8.13	1.20
1700	0.242	8.78	0.57
1800	0.256	9.34	0.41
1900	0.270	9.66	0.29
2000	0.285	9.80	0.21
2100	0.298	10.18	0.15
2200	0.312	10.49	0.11

Table 2: Masses m_G and widths Γ_G of the simulated graviton resonances, and the gaussian width of the observed resonance Γ_m after detector effects. $\sigma \cdot B$ is the cross-section times branching ratio in the test model.

m_G (GeV)	Mass window (GeV)	N_S	N_B	$N_S^{\min}$ (fb)	$(\sigma \cdot B)^{\min}$
500	± 10.46	20750	816	142.9	1.941
1000	± 18.21	814	65	40.2	0.542
1500	± 24.37	84.3	11	16.5	0.235
1700	± 26.53	38.6	5.8	12.0	0.178
1800	± 27.42	27.2	4.3	10.4	0.156
1900	± 28.29	19.2	3.2	10.0	0.152
2000	± 28.76	13.2	2.3	10.0	0.157
2100	± 30.55	9.4	1.8	10.0	0.159
2200	± 31.46	6.8	1.4	10.0	0.162

Table 3: The number of signal events in the test model, N_S, expected inside each graviton mass window in a run of $100\,\mathrm{fb}^{-1}$, after detector effects; the number of Standard Model background events, N_B; the minimum number of signal events required to detect the resonance, $N_S^{\min}$; and the minimum production cross-section times branching ratio $(\sigma \cdot B)^{\min}$ required to detect the resonance via e^+e^- production.

not included in ATLFAST. These losses are estimated in [13] to be approximately 5% at high transverse momentum if the tracks are well isolated. Our efficiency value is therefore conservative. The number of Drell-Yan background events (N_B) inside each mass window after these cuts is given in table 3.

The expected signal in the test model for $m_G = 1.5\,\mathrm{TeV}$ can be seen in figure 2, showing the data expected for $100\,\mathrm{fb}^{-1}$ of integrated luminosity. The signal is prominent above the small Standard Model background.

We now consider the model-independent detection limit for such a resonance. The minimum number of signal events, $N_S^{\min}$, needed to detect the resonance above

JHEP09(2000)019

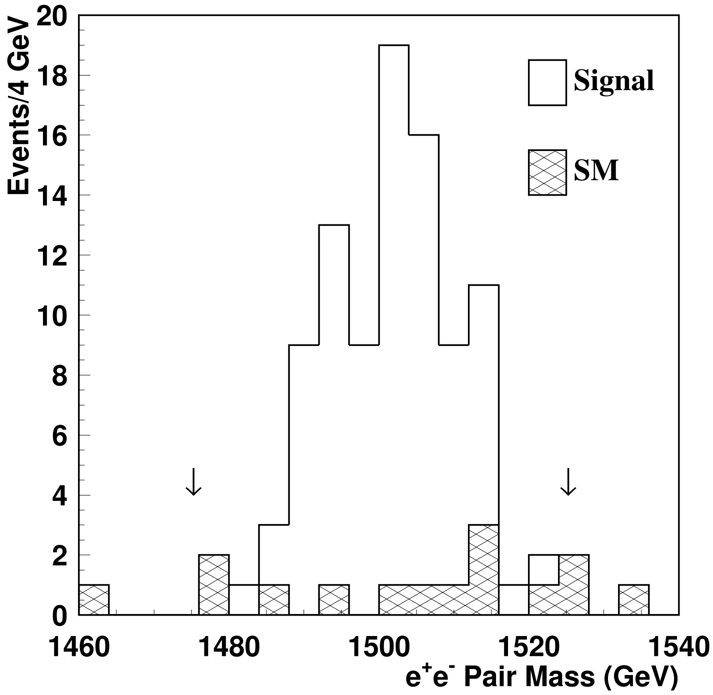

Figure 2: The number of events per 4 GeV mass bin from a graviton resonance, with $m_G = 1.5\,\mathrm{TeV}$ (signal), superimposed on the expected Standard Model background (SM), for $100\,\mathrm{fb}^{-1}$ of integrated luminosity. The mass window used to select the signal is indicated by arrows.

the background is taken to be $5\sqrt{N_B}$ or 10 events, whichever is greater, in order to ensure that the signal is statistically significant. The minimum cross-section times branching ratio required to produce this number of events is also given in table 3, after correcting for the detector acceptance and efficiency, and assuming an integrated luminosity of $100\,\mathrm{fb}^{-1}$.

It can be seen from these results that the background becomes negligible for graviton masses above 1800 GeV. It should be emphasised that these results are independent of the test model, and rely only on the assumption that the width of the resonance to be detected is negligible compared to the detector mass resolution. However, as an example, we can compare this cross-section limit with the values predicted by our test model, in order to determine the physics reach for ATLAS for this specific case. This is done in figure 3, which displays $\sigma \cdot B$ for the test model and $(\sigma \cdot B)^{\min}$. The test model could be detected for graviton masses up to 2080 GeV. Using figure 3, similar estimates of the ATLAS search reach for other models can be determined without repeating the detector simulation or background analysis. The search reach for other collider experiments, such as CMS, would require a new simulation with the appropriate mass resolution.

Our results differ from those in [13] for the case of a Z' with Standard Model couplings, both because of the acceptance difference arising from the spin of the

JHEP09(2000)019

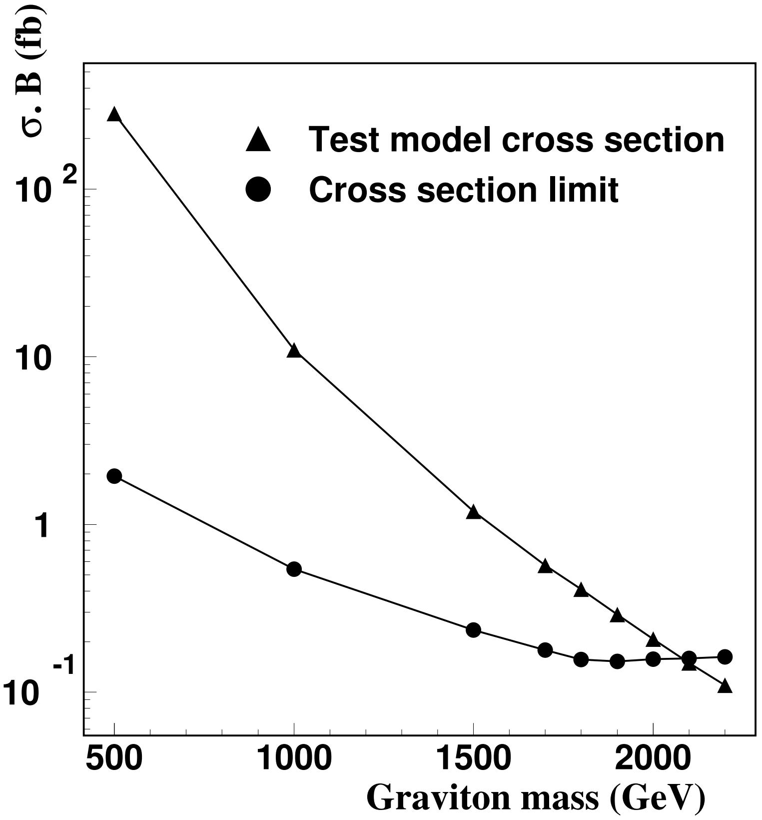

Figure 3: The cross-section times branching ratio, $\sigma \cdot B$, for $G \to e^+e^-$ in the test model and the smallest detectable cross-section times branching ratio, $(\sigma \cdot B)^{\min}$

resonance, and the Z' width, which exceeds 50 GeV for a Z' mass of 2 TeV.

4. Angular distributions

In order to demonstrate that the observed resonance is a graviton and not due to a spin-1 Z', or similar exotic object, it is necessary to show that it is produced by a spin-2 intermediate state. The strong differences between the angular distributions shown in figure 1 would allow the spin of the resonance to be determined given sufficient statistics. Information can also be gained on the relative production rate from the gg and $q\bar{q}$ processes.

Figure 4 shows the angular distribution expected in the test model for a graviton resonance mass of 1.5 TeV, after passing the events through the detector simulation and analysis cuts, using the statistics for $100\,\mathrm{fb}^{-1}$ of data. The contributions from Standard Model Background, gg production and $q\bar{q}$ production of the graviton resonance are shown. In this case, 83% of the graviton production is from the gg process. The distribution expected from a spin-1 resonance is also shown. The cutoff in the detector acceptance at $|\eta| = 2.5$ removes events at large $|\cos\theta^*|$. For heavy gravitons, which are produced with little longitudinal momentum, the effect is relatively

JHEP09(2000)019

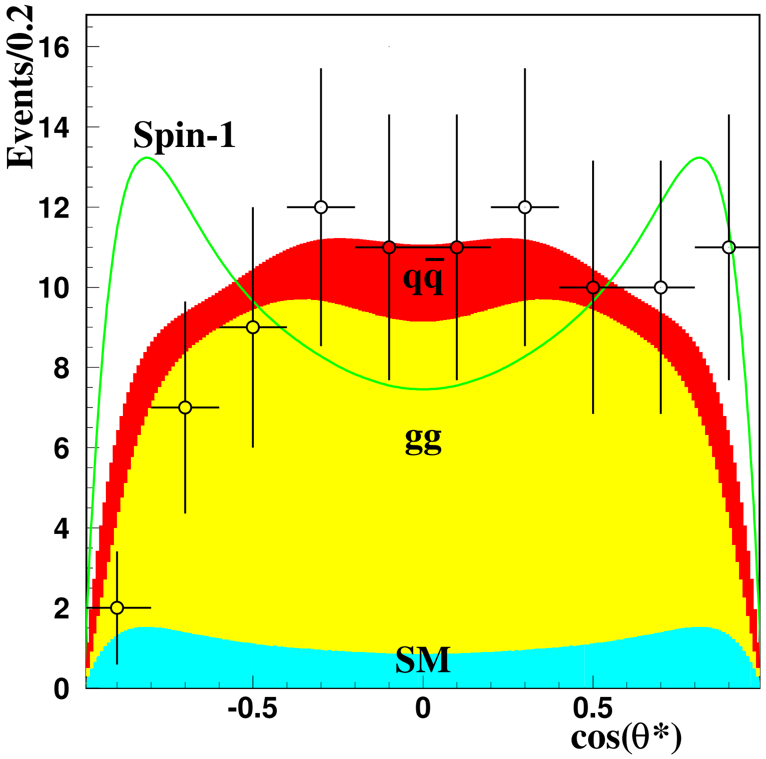

Figure 4: The angular distribution of data (points with errors) in the test model for $m_G = 1.5\,\mathrm{TeV}$ and $100\,\mathrm{fb}^{-1}$ of integrated luminosity. The stacked histograms show the contributions from the Standard Model (SM), gg production (gg) and $q\bar{q}$ production ($q\bar{q}$). The curve shows the distribution expected from a spin-1 resonance.

sharp in $\cos\theta^*$, while for lighter gravitons and Drell-Yan processes, the acceptance loss reaches to lower $|\cos\theta^*|$ values.

A likelihood function was constructed to quantify the information in the angular distributions, defined as

$$L = x_q \cdot f_q(\theta^*) \cdot A_q(M,\theta^*)/I_q(M) + x_g \cdot f_g(\theta^*) \cdot A_g(M,\theta^*)/I_g(M) + \\ + x_{\mathrm{DY}} \cdot f_{\mathrm{DY}}(\theta^*) \cdot A_{\mathrm{DY}}(M,\theta^*)/I_{\mathrm{DY}}(M)\,, \tag{4.1}$$

where x_i is the fraction of the events from each contributing process, $f_i(\theta^*)$ is the angular distribution of the process, $A_i(M,\theta^*)$ is the acceptance of the detector as a function of the mass of the electron pair and θ^*, and

$$I_i(M) = \int_{-1}^{1} f_i(\theta^*) \cdot A_i(M,\theta^*)\; d\cos\theta^*\,, \tag{4.2}$$

$i = q, g, \mathrm{DY}$ for the processes $q\bar{q} \to G$, $gg \to G$, and $q\bar{q} \to Z/\gamma^*$, respectively. Only the shape of the distribution is used in the statistical tests, and the coefficients x are constrained such that

$$x_q + x_g + x_{\mathrm{DY}} = 1\,. \tag{4.3}$$

JHEP09(2000)019

m_G	$N_S^{\min}$			$\sigma \cdot B$ (fb)		
(GeV)	90% CL	95% CL	99% CL	90% CL	95% CL	99% CL
500	140	141	226	1.90	1.92	3.07
1000	59	70	99	0.80	0.94	1.33
1500	43	48	70	0.61	0.68	1.00
1700	41	48	65	0.61	0.71	0.96
1800	29	33	58	0.43	0.49	0.87
1900	32	40	64	0.49	0.61	0.98
2000	36	41	69	0.56	0.64	1.08
2100	31	45	59	0.49	0.71	0.93
2200	29	33	55	0.45	0.52	0.86

Table 4: The minimum numbers of signal events, $N_S^{\min}$, needed to distinguish the spin-2 and spin-1 hypotheses at 90, 95 and 99% confidence, and the corresponding cross-section times branching ratio, for a run of $100\,\mathrm{fb}^{-1}$.

In order to evaluate the discovery reach of the experiment, in terms of its ability to reveal the spin-2 nature of the resonance, the following procedure was followed, intended to mimic an ensemble of possible experimental runs:

1. N events were generated, containing the expected number N_{DY} background events, with a Poisson distribution, and the remainder being graviton resonance decays with the $q\bar{q}$ and gg mixture of the test model at that mass point.

2. $-\log L$ was evaluated for two hypotheses:

   (a) $x_q = x_g = 0$, $x_{\mathrm{DY}} = 1$, corresponding to a spin-1 resonance, such as a Z'

   (b) all the coefficients set to the values in the test model with the expected Standard Model background fraction.

3. N was increased by adding graviton resonance events, until the difference in $-\log L$ between the two hypotheses reached 1.34, then 1.92 and finally 3.32. At these points the spin-1 hypothesis can be eliminated with 90, 95 and 99% confidence, respectively.

4. This procedure was repeated for many sets of events, and the average value of N needed for discrimination was found for each confidence level.

This value of N provides a measure of the statistics needed in a typical experiment in order to determine the spin-2 nature of the resonance. $N_S^{\min} = N - N_{\mathrm{DY}}$ is the number of signal events in the sample at the confidence limit. Table 4 shows results of this procedure. The 90% confidence limit for $m_G = 500\,\mathrm{GeV}$ is raised by the requirement that the sample contains at least $5\sqrt{N_{\mathrm{DY}}}$ signal events. In this case, less

JHEP09(2000)019

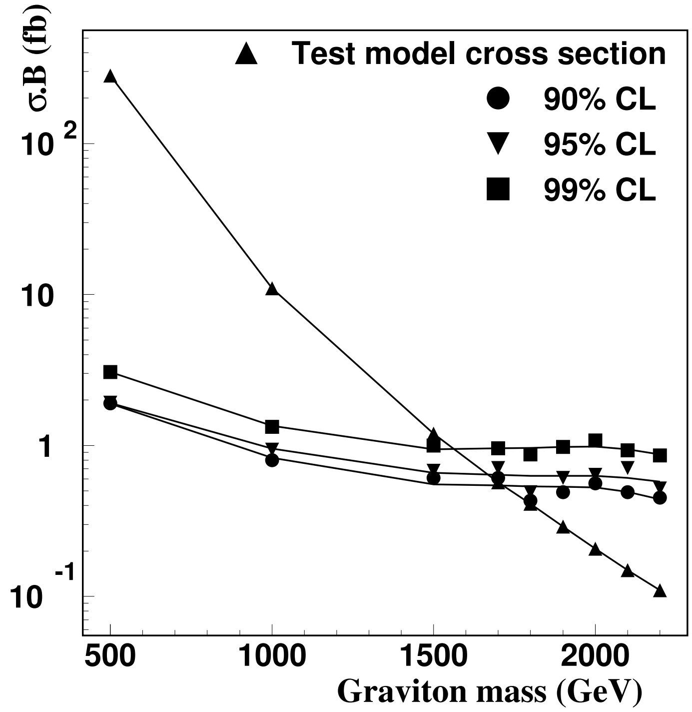

Figure 5: The smallest cross-section times branching ratio for which the spin-2 hypothesis is favoured over the spin-1 hypothesis at 90, 95 and 99% confidence. The cross-section times branching ratio of the test model is also shown.

events would be sufficient to establish the spin of the resonance, but would not meet our criterion for a discovery. At very high m_G, the discrimination becomes more difficult because of the increased fraction of the resonance production coming from the $q\bar{q}$ initial state.

Figure 5 shows the confidence limit curves and the corresponding cross-section times branching ratio in our test model. Smooth curves have been drawn through the points since some statistical fluctuations remain at high mass. These results are model independent, as long as the assumption that the coupling of the graviton resonance is univeral holds true. This assumption affects the fraction of graviton resonance production from gg and $q\bar{q}$ initial states, and hence the shape of the angular distribution. The cross-section times branching ratio of the test model is shown for comparison. In this model, the spin of the resonance could be determined with 90% confidence for graviton resonance masses as high as 1720 GeV.

5. Conclusions

The discovery limits for the detection of the decay mode $G \to e^+e^-$, derived above, show that the resonance can be detected up to a graviton resonance mass of 2080 GeV in our test model. The limits are model independent as long as the graviton cou-

JHEP09(2000)019

plings are universal and give rise to narrow resonances, with widths less than the experimental resolution. The angular distribution of the lepton pair can be used to determine the spin of the state. In our test model, the angular distribution favours a spin-2 hypothesis over a spin-1 hypothesis at 90% confidence for graviton masses up to 1720 GeV. Once the spin of the resonance has been determined, it will be useful to check the universality of its couplings [14]. Muon and jet production cross-sections in the resonance region as well as decays into photons, massive vector bosons, higgs bosons and top quarks could be used to check this universality. The bosonic final states would provide a further test of the spin, since their angular distributions will be different from that of the electrons considered above. They would also serve to rule out other models of high mass resonances. For example, the Z' will not couple to a two photon final state.

Acknowledgments

We would like to thank J. March-Russell for an interesting discussion and I. Vernon for helpful discussions on different scenarios. MAP would like to thank C.G. Lester for his technical help. This work was funded by the U.K. Particle Physics and Astronomy Research Council.

References

[1] L. Randall and R. Sundrum, *A large mass hierarchy from a small extra dimension*, *Phys. Rev. Lett.* **83** (1999) 3370 [hep-ph/9905221].

[2] L. Randall and R. Sundrum, *An alternative to compactification*, *Phys. Rev. Lett.* **83** (1999) 4690 [hep-th/9906064];
C. Csáki and Y. Shirman, *Brane junctions in the Randall-Sundrum scenario*, *Phys. Rev.* **D 61** (2000) 024008 [hep-th/9908186];
J. Lykken and L. Randall, *The shape of gravity*, *J. High Energy Phys.* **06** (2000) 014 [hep-th/9908076];
I. Oda, *Mass hierarchy from many domain walls*, *Phys. Lett.* **B 480** (2000) 305 [hep-th/9908104]; *Mass hierarchy and trapping of gravity*, *Phys. Lett.* **B 472** (2000) 59 [hep-th/9909048];
T.J. Li, *Non-compact AdS_5 universe with parallel positive tension 3-branes*, hep-th/9911234;
N. Arkani-Hamed, S. Dimopoulos, G. Dvali and N. Kaloper, *Infinitely large new dimensions*, *Phys. Rev. Lett.* **84** (2000) 586 [hep-th/9907209];
I.I. Kogan, S. Mouslopoulos, A. Papazoglou, G.G. Ross and J. Santiago, *A three three-brane universe: new phenomenology for the new millennium?*, *Nucl. Phys.* **B 584** (2000) 313 [hep-ph/9912552].

JHEP09(2000)019

[3] H. Davoudiasl, J.L. Hewett and T.G. Rizzo, *Phenomenology of the Randall-Sundrum gauge hierarchy model*, *Phys. Rev. Lett.* **84** (2000) 2080 [hep-ph/9909255].

[4] N. Arkani-Hamed, S. Dimopoulos and G. Dvali, *The hierarchy problem and new dimensions at a millimeter*, *Phys. Lett.* **B 429** (1998) 263 [hep-ph/9803315];
E. Accomando, I. Antoniadis and K. Benakli, *Looking for TeV-scale strings and extra-dimensions*, *Nucl. Phys.* **B 579** (2000) 3 [hep-ph/9912287];
I. Antoniadis, K. Benakli and M. Quiros, *Direct collider signatures of large extra dimensions*, *Phys. Lett.* **B 460** (1999) 176 [hep-ph/9905311];
L. Vacavant and I. Hinchcliffe, *Model independent extra-dimension signatures with ATLAS*, hep-ex/0005033.

[5] G. Marchesini, B.R. Webber, G. Abbiendi, I.G. Knowles, M.H. Seymour and L. Stanco, Herwig*: a Monte Carlo event generator for simulating hadron emission reactions with interfering gluons. Version 5.1 - april 1991*, *Comput. Phys. Commun.* **67** (1992) 465;
G. Corcella et al., *Herwig 6.1 release note*, hep-ph/9912396.

[6] E. Richter-Was, D. Froidevaux and L. Poggioli, *ATLFAST 1.0 A package for particle-level analysis*, ATLAS Internal Notes ATL-PHYS-96-079 (1996) and ATL-PHY-98-131 (1998).

[7] H. Davoudiasl, J.L. Hewett and T.G. Rizzo, *Experimental probes of localized gravity: on and off the wall*, hep-ph/0006041.

[8] T. Han, J.D. Lykken and R.-J. Zhang, *On Kaluza-Klein states from large extra dimensions*, *Phys. Rev.* **D 59** (1999) 105006 [hep-ph/9811350].

[9] G.F. Giudice, R. Rattazzi and J.D. Wells, *Quantum gravity and extra dimensions at high-energy colliders*, *Nucl. Phys.* **B 544** (1999) 3 [hep-ph/9811291].

[10] J.L. Hewett, *Indirect collider signals for extra dimensions*, *Phys. Rev. Lett.* **82** (1999) 4765 [hep-ph/9811356].

[11] H. Murayama, I. Watanabe and K. Hagiwara, HELAS*: HELicity Amplitude Subroutines for Feynman Diagram Evaluations*, KEK Report 91–11, January 1992.

[12] D.L. Rainwater, private communications;
T. Han, D. Rainwater and D. Zeppenfeld, *Drell-Yan plus missing energy as a signal for extra dimensions*, *Phys. Lett.* **B 463** (1999) 93 [hep-ph/9905423].

[13] *ATLAS detector and physics performance technical design report*, CERN/LHCC/99-15, ATLAS TDR 14, 25 May 1999.

[14] B.C. Allanach, K. Odagiri, M.A. Parker and B.R. Webber, work in progress.

JHEP09(2000)019